Characterization of Fluorescent Phospholipid Liposomes Entrapped in Sol−Gel Derived Silica

Travis Besanger, Ying Zhang, and John D. Brennan*

Department of Chemistry, McMaster University, 1280 Main Street West, Hamilton, ON, L8S 4M1 Canada

Received: June 21, 2002; In Final Form: August 8, 2002

Bilayer lipid membranes (BLMs) have been widely examined as sensing elements for a variety of analytes, in both the vapor and solution phases, using electrochemical, acoustic wave, and fluorescence methods. For successful development of stable sensing devices, it is necessary to be able to immobilize the BLMs in a manner that allows long-term retention of the membrane structure and still permits large-scale structural reorganizations such as phase transitions. In this work, small unilamellar liposomes were formed from either 1,2-dipalmitoyl-*sn*-glycero-3-phosphocholine (DPPC) or L-a-phosphatidylcholine (egg PC) and were doped with 1−5 mol % of the fluorescent probes diphenylhexatriene (DPH) or nitrobenzoxadiazole-labeled dipalmitoylphosphatidylethanolamine (NBD-PE). The liposomes were entrapped in a series of different sol−gel derived silicate materials and the stability and phase-transition behavior of the liposomes was characterized. DPPC was observed to undergo reversible phase transitions when entrapped in glasses derived from either sodium silicate or a diglyceryl silane precursor; however, liposomes did not undergo phase transitions when entrapped in tetraethyl orthosilicate derived glasses, indicating that they had likely ruptured during the encapsulation process. As a practical demonstration of the use of the immobilized membranes for sensing applications, we have examined the use of pH-induced phase transitions as a means of generating a fluorescence signal that is based on changes in self-quenching of NBD-PE within liposomes composed of DPPC and dipalmitoylphosphatidic acid (DPPA). The results show that such pH-induced phase transitions occur for the entrapped vesicles and that the fluorescence responses follow the pH dependence of DPPA.

Introduction

The immobilization of intact bilayer lipid membranes (BLMs) has received a considerable amount of attention in recent years owing to their potential use for the development of new analytical technologies such as biosensors, affinity chromatography, and high-throughput drug screening.[1−10] The practical utility of BLMs for these applications has been further extended through the incorporation of various elements within the membrane. Such species include conductive moieties such as ferrocene[11] and buckminsterfullerenes (C_{60}),[12,13] which make an otherwise electrically insulating structure excitable, and the insertion of integral membrane proteins to allow for selective electrochemical[14−16] or optical[17,18] changes in response to their analytes. In each case, the stability of the device depends on the successful immobilization of the membrane and its constituents onto a solid support, and in many cases requires that the membrane retain the ability to undergo phase transitions[19] or transmembrane ion channel activity.[14,16]

A number of strategies have been reported for the immobilization of bilayer lipid membranes, including supporting of BLMs on the pores of filter paper,[20] covalent attachment of monolayer or bilayer lipid membranes to surfaces,[1,3,4,21] tethering of phospholipid liposomes to a surface by deposition,[22] covalent attachment[23] or attachment via avidin−biotin linkages,[24] and entrapment of BLMs into polymer multilayers to provide a semihydrated internal surface to allow incorporation or bulkier membrane receptors and proteins.[4] The dynamic and physical properties of such BLMs have been examined using a variety of techniques such as voltammetry,[25−28] electrostriction,[29] electrical impedance spectroscopy,[30,31] and fluorescence spectroscopy.[32] Such studies have shown that there are several limitations related to the use of supported BLMs as practical devices due to the intrinsic fragility of the membrane and the generally harsh nature of the immobilization methods employed. Problems arise due to the coupling of the lipid bilayer to the solid support, which can produce an unstable structure with a lifetime that is too short for functional purposes. Furthermore, the structure of intrinsic membrane proteins relies on hydrophobic interactions internal to the lipid bilayer, as well as hydrophilic interactions on either side of the lipid membrane.[4] Very often with conventional supported BLMs, what would be considered the hydrophilic interior surface for the membrane protein is replaced by the solid substrate.[4,33] This results in destabilization of the membrane protein with a concomitant loss in activity, or in the worst-case scenario complete loss of activity due to full denaturation of the protein. These issues have been partially addressed by covalent attachment of a lipid monolayer to a solid substrate, which alleviates membrane dissociation; however, this method does not address the second issue mentioned, and furthermore decreases the natural dynamic behavior of the bilayer.[3,4]

An emerging method for the immobilization of biological species is their entrapment within inorganic matrixes formed by the sol−gel processing method.[34,35] The method involves the formation of a colloidal sol solution resulting from the hydrolysis of suitable silane precursors such as tetramethyl orthosilicate (TMOS) or tetraethyl orthosilicate (TEOS). A

* To whom correspondence should be addressed. Tel: (905) 525-9140 (ext. 27033). Fax: (905) 527-9950. E-mail: brennanj@mcmaster.ca. Internet: http://www.chemistry.mcmaster.ca/faculty/brennan.

10.1021/jp0263525 CCC: $22.00
Published on Web 09/20/2002

buffered aqueous solution containing the biological reagent of interest is added to the sol to initiate a rapid polycondensation reaction, which produces a hydrated gel that effectively entraps the species without the need for tethering to a solid surface. This immobilization method has already been proven to be advantageous for the incorporation of biological species such as soluble proteins and has been used as a platform for optical sensing and other analytical purposes.[35] However, the sol−gel method has found much less use in the area of membrane immobilization. In fact, only a few reports exist describing the immobilization of BLMs or membrane-bound proteins into inorganic silica matrixes formed by the sol−gel method,[36−39] and investigations of the physical properties of these entrapped liposomes have yet to be presented. Aspects such as the stability, dynamics and phase-transition behavior of entrapped liposomes have not been examined, thus it is not clear if entrapped liposomes are free to move within the cavity that entraps them, or if they retain their dynamic properties. Such factors are critically important as they will impact on the use of entrapped membranes as sensing elements and may determine the stability of membrane-bound receptors upon entrapment.

In this study we have entrapped phosphatidylcholine and mixed phospthatidylcholine:phosphatidic acid liposomes into sol−gel derived silica prepared from TEOS, sodium silicate, or a newly synthesized diglycerylsilane precursor and have used fluorescence methods to examine the integrity and phase-transition behavior of the entrapped liposomes as a function of aging of the silica. Some liposomes were composed of pure dipalmitoylphosphatidylcholine (DPPC) to produce a system with a phase-transition temperature above room temperature (T_m = 42 °C[40]), whereas others were composed of egg PC to provide a system with a phase transition below room temperature (T_m < 0 °C). Other liposomes were prepared from a mixture of DPPC and dipalmitoylphosphatidic acid (DPPA) to produce pH dependent liposomes for studies of pH-induced phase transitions.

The fluorescent probes 1,6-diphenyl-1,3,5-hexatriene (DPH) and nitrobenzoxadiazole-labeled phosphatidylethanolamine (NBD-PE) were incorporated into BLMs at levels of 1−5 mol % to probe the dynamics and phase-transition behavior of liposomes via changes in emission intensity, fluorescence lifetimes, and fluorescence anisotropy. The results clearly show that entrapment into silica can have a significant effect on the behavior of liposomes and that careful selection of sol−gel precursors is critically important in ensuring that liposomes are entrapped in a functional manner. As a practical demonstration of the use of the immobilized membranes for sensing applications, we have examined the use of pH-induced phase transitions as a means of generating a fluorescence signal that is based on changes in self-quenching of NBD-PE within liposomes composed of DPPC and DPPA.[41] The results show that such pH-induced phase transitions occur for the entrapped vesicles and that the fluorescence responses follow the pH dependence of DPPA.

Experimental Section

Materials. 1,2-Dipalmitoyl-*sn*-glycero-3-phosphocholine (DPPC), L−a-phosphatidylcholine (egg PC), and 1,2-dipalmitoyl-*sn*-glycero-3-phosphatidic acid (DPPA) were purchased from Avanti Polar-Lipids, Inc, (Alabaster, AL). The fluorescent probes; 1,6-diphenyl-1,3,5-hexatriene (DPH) and *N*-(7-nitrobenz-2-oxa-1,3-diazol-4-yl)-1,2-dihexadecanoyl)-*sn*-glycero-3-phosphoethanolamine, triethylammonium salt (NBD-PE), were purchased from Molecular Probes (Eugene, OR). Sodium silicate solution (technical grade, 9.1% sodium oxide, 29.2% silica, amorphous, 61.7% water) was purchased from Fisher Scientific (Toronto, ON). Tetraethyl orthosilicate (TEOS, 99.999%) was purchased from Aldrich (Milwaukee, WI). Diglycerylsilane (DGS) was provided by Dr. Michael Brook of McMaster University and was prepared by a method described elsewhere.[42] Polymethacrylate fluorometer cuvettes (transmittance curve C) were obtained from Sigma (St. Louis, MO). All water was twice distilled and deionized to a specific resistance of at least 18 MΩ·cm using a Milli-Q Synthesis A10 water purification system. All other chemicals were of analytical grade and were used without further purification.

Methods. *Entrapment of Liposomes.* Phospholipid, DPH, and NBD-PE stock solutions were prepared in chloroform and were mixed in the appropriate molar ratios in disposable glass vials. The chloroform was removed by evaporation under a dry nitrogen gas stream to remove the bulk of the organic solvent, followed by evaporation under vacuum for 2 h. The resulting dried lipid films were then rehydrated in the appropriate buffer followed by high frequency sonication for $2^1/_2$ h with a VWR Scientific Aquasonic Model 50T sonicator to create small multilamellar phospholipid vesicles. The resulting phospholipid solutions that were used for steady-state and time-resolved fluorescence studies consisted of 20:1 (mol:mol) DPPC or egg PC to DPH hydrated to final concentrations of 1.4 μM and 71 nM, respectively, in 50 mM Tris−HCl buffer pH 7.4. Liposome samples used for fluorescence microscopy were composed of 1.5 mol % NBD-PE/DPPC hydrated to final concentrations of 1 and 70 μM, respectively, in 10 mM HEPES containing 100 mM KCl. In this case, the sample was sonicated for 10 min to remove the lipid from the sides of the glass vial and then left to hydrate overnight to create large liposomes.

Preparation of TEOS derived materials was done by sonicating a mixture of 4.5 mL of TEOS, 1.4 mL of distilled deionized water, and 100 μL of 0.1N HCl for 1 h at ambient temperature until the mixture was clear and monophasic. The resulting solution was mixed in a 1:1 volume ratio with a buffered aqueous solution of liposomes and allowed to stand until gelation occurred. The sodium silicate derived materials were prepared according to the method described by Bhatia et al.[43] Briefly, a 22.8% (w/w) solution of stock sodium silicate in distilled deionized water was prepared. A strongly acidic DOWEX cation-exchange resin was added to bring the pH of the solution to approximately 4, by preparing a slurry of 28% (w/w) diluted sodium silicate solution to resin. The resulting slurry was then vacuum filtered to remove the resin and collected in a glass vial that was then mixed in a 1:1 volume ratio with a buffered aqueous solution of liposomes and allowed to stand until gelation occurred. Diglycerylsilane (DGS) derived sol−gels were prepared by adding 0.212 g of DGS and 5 μL of 0.1 N HCl to 650 μL of distilled deionized water followed by sonication at 0 °C for 1.5 h until all the silane precursor was dissolved and the solution had become homogeneous and transparent. The resulting solution was mixed in a 1:1 volume ratio with the liposome solution to promote gelation.

In all cases, gelation commenced shortly after mixing the silane precursor and the liposome solution in a disposable polymethacrylate cuvette to produce a transparent or semitransparent glass. Following gelation, the monolithic sols were aged in the presence of buffer (wet aging) or in air (dry aging) for up to 60 days with the cuvette covered with Parafilm at room temperature.

Steady-State Fluorescence Measurements. Fluorescence measurements were performed by using either a SLM 8100 spectrofluorometer (Spectronic Instruments, Rochester, NY), or a Cary Eclipse spectrofluorometer. Samples containing DPH

were excited at 337 nm with emission collected from 350 to 600 nm. Emission spectra of NBD-PE-doped liposomes was collected from 485 to 600 nm with an excitation wavelength of 463 nm. All spectra were collected in 1 nm increments using 4 or 5 nm band-passes on the excitation and emission monochromators and an integration time of 0.3 s per point. Appropriate blanks were subtracted from each sample and the spectra were corrected for the wavelength dependence of the emission monochromator and photomultiplier tube.

Steady-state fluorescence anisotropy measurements were performed in the L-format on the SLM 8100 instrument. Single point fluorescence anisotropy measurements of DPH-doped liposomes were generally made at an emission wavelength of 452 nm, with excitation at 337 nm, unless otherwise stated. All fluorescence anisotropy values were corrected for the instrumental *G* factor to account for any polarization bias in the monochromators. All fluorescence anisotropy values reported are the average of five measurements each on two different samples. Temperature-dependent anisotropy studies utilized a NESLAB ENDOCAL water-bath and a HANNA Instruments HI 9043 microcomputer thermocouple thermometer to control and measure the temperature of the entrapped liposome samples as the temperature was varied from 20 to 70 °C.

Time-Resolved Fluorescence. Time-resolved fluorescence intensity and anisotropy decay data was acquired in the time domain using an IBH 5000U time-correlated single photon counting fluorometer, as described elsewhere.[44] A pulsed ultraviolet light-emitting diode operating at a 1 MHz repetition rate with a 1.3 ns pulse duration and a wavelength of 370 nm was used for excitation of the dye. The intensity decay data were collected under magic angle polarization conditions, passed through a monochromator (16 nm band-pass) and detected on a TBX-04 PMT detector. Single point intensity or anisotropy decay data were collected at 452 nm. Intensity decay data were collected into 1024 channels (50 ps per channel) until 10 000 counts were obtained in the peak channel. The instrument response function was collected by measuring the Rayleigh scattering of the laser pulse from water (typical fwhm of 1.3 ns) and was used to deconvolute the instrument response profile from the experimentally determined decay trace. Appropriate time-shift parameters were obtained by allowing this to be a floating parameter in the fit.

The function describing the fluorescence intensity decay was fit to a sum of exponentials according to the equation[45]

$$I(t) = \sum_i \alpha_i \exp(-t/\tau_i) \tag{1}$$

where τ_i is the decay time of the *i*th component and α_i is the preexponential factor. The goodness-of-fit was determined using the reduced χ^2 parameter and by visual inspection of residual plots.[46] The fractional fluorescence of component *i* (f_i) was calculated from

$$f_i = (\alpha_i\tau_i/\sum_i \alpha_i\tau_i) \tag{2}$$

The intensity-weighted mean lifetime values, $\langle\tau\rangle$, were obtained from single point decay data at 452 nm emission using the following equation:

$$\langle\tau\rangle = \sum_i f_i\tau_i \tag{3}$$

Time-resolved decays of fluorescence anisotropy were constructed from intensity decays that were obtained using vertically polarized excitation and vertically polarized emission (I_{VV}) or horizontally polarized emission (I_{VH}) and were corrected for the instrument response profile and the instrumental *G* factor, as described in detail elsewhere.[47−50] The anisotropy decay data were fit to the expression

$$r(t) = \left[\frac{r_\infty}{r_o} + \left(1 - \frac{r_\infty}{r_o}\right)e^{-t/\phi}\right]r_o \tag{4}$$

where $r(t)$ is the time-dependent anisotropy, r_o is the limiting anisotropy, r_∞ is the residual anisotropy at infinite time, and ϕ is the rotational correlation time. The ratio of the limiting and residual anisotropy values may be used to extract the maximum semiangle (θ_{max}) for rotation of the probe within the bilayer lipid membrane according to

$$\cos^2\theta_{max} + \cos\theta_{max} = 2\sqrt{\frac{r_o}{r_\infty}} \tag{5}$$

The value of θ_{max} will vary from zero, indicative of completely restricted motion up to 90° for a completely mobile probe.

Leaching Studies. Liposomes containing the fluorescent probe NBD-PE entrapped in the three types of sol−gel derived materials and were wet aged in buffers of different pH over a period of several weeks. Every few days the fluorescence emission from the surrounding buffer solution was monitored for NBD-PE fluorescence to determine if any leaching had occurred.

Confocal Fluorescence Microscopy. Micrographs were obtained using a Carl Zeiss LS 510 laser scanning microscope with a CAPROMAT 64X water immersion objective. Excitation was achieved using a Lasos Ar^+ laser operating at 488 nm with an output power of 15 mW and a spot size of approximately 0.5 μm. The typical field of view was 150 μm × 150 μm unless otherwise stated. All images were saved as jpg files and were processed off-line.

pH Sensitive Liposomes. Phospholipid liposomes used for signaling changes in pH were prepared by mixing a molar ratio of 85% DPPC/10% DPPA/5% NBD-PE and hydrating the mixture in 10 mM HEPES, 100 mM KCl pH 7.4 buffer to a final concentration of 1.19 mM:0.14 mM:0.07 mM, respectively. The samples were allowed to age dry overnight at room temperature. The buffer was exchanged twice for each sample every 36 h for 3 days by applying 1 mL of 100 mM phosphate buffer at pH 1.31, 3.28, 4.75, 5.36, 6.36, 7.08, 7.73, 7.89, 8.51, or 10.27 to the top of the sample in a small-volume polymethacrylate cuvette, and the fluorescence intensity of the NBD-PE was monitored as a function of pH.

Results and Discussion

Leaching of Phospholipid Liposomes. The use of phospholipid liposomes to reduce the leaching of encapsulated fluorescent dyes from sol−gel monoliths has been reported by Nguyen et al.[39] A significant reduction in leaching of fluorescent probe was reported due to its encapsulation inside the phospholipid liposome. To address the question of whether any lipid leaches from the sol−gel monolith, phospholipid liposomes containing the fluorescently labeled lipid NBD-PE were prepared and were wet aged over a period of several weeks. Examination of the surrounding buffer solution indicated that no leaching of lipid occurred at any time when aging was done in the pH range between 3 and 9. Aging of the material at extreme pH values

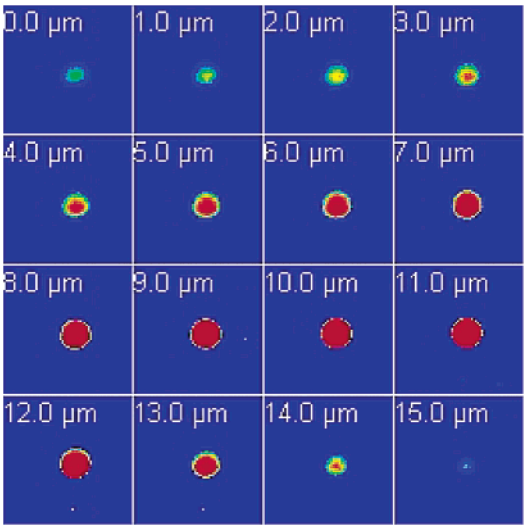

Figure 1. Confocal fluorescence image of 2.5% NBD-PE labeled DPPC phospholipid vesicles entrapped in a sol−gel thin film composed of diglyceryl silane. The lipid concentration is 70 μM. White numbers indicate the depth of the confocal image. Images are 60 μm × 60 μm.

(pH < 3 or pH > 9) did result in moderate increases in the emission intensity of the surrounding buffer as aging proceeded; however, visible degradation of the silica was observed for these samples and thus the fluorescence can be attributed to release of phospholipids to the solution as a result of dissolution of the matrix. On the basis of these findings, all studies of entrapped liposomes were done under neutral pH conditions unless otherwise stated.

Confocal Fluorescence Microscopy. As a first step to examine whether the liposomes were entrapped in an intact state, large DPPC liposomes were prepared that contained 2.5 mol % of NBD-PE, and the vesicles were entrapped in DGS derived silica that was spin cast as a thick film on a glass microscope slide (film thickness was ~30 μm). Imaging of the films containing 70 μM of the entrapped liposomes was done using a 64× water immersion lens, and clearly revealed the presence of spherical liposome structures, as shown in Figure 1. Depth-resolved confocal imaging shows the liposome structure as a function of the depth of the focal plane and reveals that the diameter of the liposome grows to a maximum diameter of ~20 μm and then contracts, as one would expect when slicing through a sphere. Similar images could be obtained for sodium silicate and TEOS derived materials, suggesting that at least some spherical liposomes were entrapped in each case. Figure 2 shows some of the other structures that were revealed by confocal imaging, including clusters of liposomes and long tube-like structures up to and over 20 μm wide and 100 μm long, which may be local regions of vesicle fusion. It should be noted that the presence of PE can promote the formation of hexagonal phases that lead to vesicle fusion.[51] However, our liposomes contained only 2.5 mol % of PE in DPPC, and thus are not likely to form hexagonal phases, particularly at the low temperature and high water content was used in this study.[52] Overall, the results show that a range of structures may be entrapped within the silica matrix and that at least a fraction of these are likely to be intact spherical liposomes.

A series of images were also collected from samples containing a concentration of 1.4 mM of lipid (20-fold higher concentration) to more accurately reflect the concentrations used for the fluorescence studies described below. Figure 3 shows the image of a DGS film containing DPPC liposomes that contained 2.5 mol % of NBD-PE. The image clearly shows that

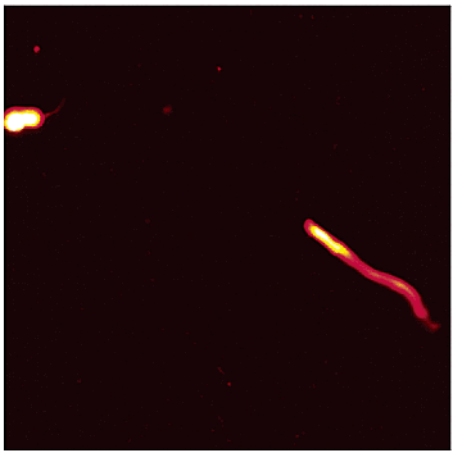

Figure 2. Confocal image of DPPC vesicles in DGS glasses showing elongated structures that suggest the formation of liposomal aggregates or bicelles. The lipid concentration is 70 μM. The image field is 60 μm × 60 μm.

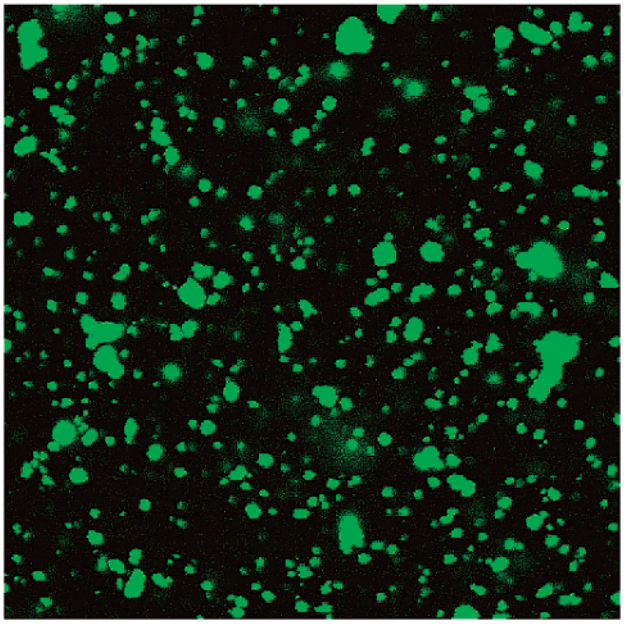

Figure 3. Confocal fluorescence image of 2.5% NBD-PE labeled DPPC phospholipid vesicles entrapped in sol−gel thin film composed of diglyceryl silane. The lipid concentration used is 1.4 mM. The image field is 150 μm × 150 μm.

there is a broad distribution of structures covering the range from <1 μm to >10 μm. The structures are predominantly spherical in shape, although there are a few irregular structures that may be clusters of liposomes or vesicle fusion products. There are ~350 individual structures within the image (150 μm × 150 μm), leading to a number density of ca. 15 000 liposomes per square millimeter. Images of other films derived from sodium silicate or TEOS were essentially identical to those of the DGS film, suggesting that all films provided good dispersion of the liposome within the matrix. It must be noted that the images are not able to differentiate between intact and disrupted liposomes, and thus it is not possible to correlate specific structures to liposome survival. For this reason, fluorescence methods were used to probe vesicle phase transitions as a means of assessing the extent of vesicle survival.

Steady-State Fluorescence Studies of Sol−Gel-Entrapped Liposomes. To more fully explore the question of whether the entrapped BLMs remained intact, and to examine the dynamic behavior of the liposomes as a function of the precursor used

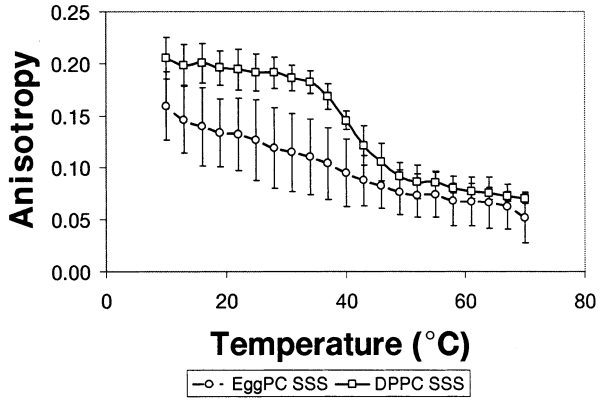

Figure 4. Changes in steady-state anisotropy with temperature of DPH within DPPC (□) and egg PC (○) liposomes upon entrapment in sodium silicate derived glass.

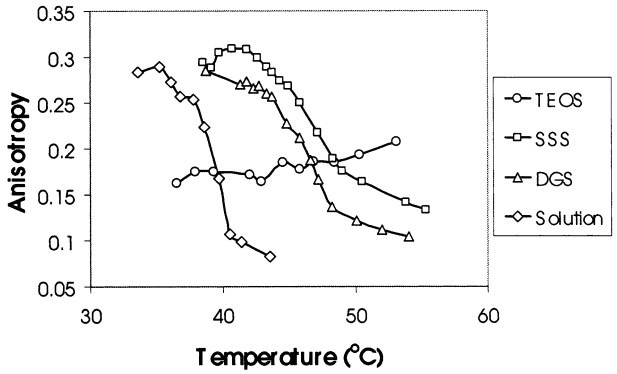

Figure 5. Comparison of phase-transition behavior measured by the steady-state anisotropy of DPH in phospholipid vesicles composed of DPPC following entrapment various sol−gel derived materials.

for entrapment, the steady-state fluorescence anisotropy of DPH was used to monitor the phase-transition behavior of DPPC and egg PC liposomes in solution and when entrapped in TEOS, DGS, and sodium silicate derived silica. Figure 4 shows the DPH anisotropy as a function of temperature for DPPC and egg PC entrapped in sodium silicate derived materials. The changes in DPH anisotropy are sigmoidal for entrapped DPPC, showing a slight decrease upon heating from 10 to 32 °C owing to slight increases in DPH mobility as the temperature increased. At 32 °C the anisotropy decreases abruptly and then levels off at approximately 50 °C, indicative of the gel-to-liquid crystalline phase transition. At this point the melting of the membrane to a more disordered liquid crystalline phase causes DPH to exhibit gauche kinks in the hexatriene chain and thus become more mobile.[32,53−55] At temperatures beyond 50 °C the anisotropy levels off again and shows slight decreases owing to increasing mobility of DPH with temperature. The results suggest a phase-transition temperature of approximately 42 °C (for samples that were aged 2 days), in excellent agreement with the expected phase-transition temperature of DPPC in solution (42 °C).[40]

The changes in anisotropy for entrapped egg PC showed only a linear decrease in anisotropy with temperature owing to temperature-induced increases in the mobility of the acyl chains within the membrane. Egg phosphatidylcholine is composed of a mixture of phospholipids whose gel phase transition is below 0 °C.[40] Thus, egg PC liposomes are expected to show no phase transitions over the temperature range studied in this work, as observed. The egg PC results provide a useful control to ensure the significant changes in anisotropy observed for entrapped DPPC liposomes are due to the lipid bilayer and not other factors such as surface adsorption or alterations in the properties of the silica matrix. The results clearly demonstrate that DPH fluorescence can accurately report on the phase-transition behavior of entrapped vesicles, setting the stage for more detailed studies of the effects of entrapment on the behavior of DPPC liposomes.

Figure 5 shows the changes in DPH anisotropy for free and entrapped DPPC liposomes after one day of aging. In solution, the changes in anisotropy occur in two steps, the first corresponding to a pretransition at a temperature of approximately 35 °C, and the second corresponding to the main phase transition at 39 °C, which is in excellent agreement with the literature value.[40] The changes in the anisotropy of DPH in sodium silicate and DGS derived silica also show clear evidence of a phase transition; however, the phase-transition temperature for DPPC in these materials was shifted to a higher temperature than was observed in solution. For example, the phase-transition temperature of DPPC entrapped in DGS derived silica was 46 °C, whereas the value in sodium silicate derived glasses was observed at 47 °C. The increase in the phase-transition temperature upon entrapment is similar to that observed for the thermal unfolding of entrapped proteins.[56−58] In the latter case, the increase in unfolding temperature has been shown to be related to excluded volume effects wherein the confinement of the entrapped protein results in a decrease in the volume available for the unfolded protein to occupy, leading to a higher free energy and hence higher temperature for unfolding.[59,60] Such an effect is also likely to be at work in the case of entrapped liposomes, where the confinement of the liposome within the pores of the silica matrix leads to the need for a greater energy input to cause the phase transition.

The reversibility of the phase transitions was examined by cooling the samples back to 20 °C to confirm that the changes in anisotropy were related to phase transitions and were not due to rupturing of the entrapped liposomes. The DPPC:DPH liposomes showed a distinct liquid crystalline to gel phase transition at 43 °C in DGS and at 42 °C in sodium silicate derived materials. The slightly lower temperature for the reverse transition is expected on the basis of the well-known hysteresis effects that occur in the phase transitions of lipid membranes.[61] It is worth noting that the final anisotropy value obtained upon cooling the sample to 20 °C was always somewhat lower than the original value measured at 20 °C before the heating−cooling cycle (typical differences were on the order of 0.05 anisotropy units). This result suggests that a fraction of the liposomes either ruptured or adsorbed to the silica at high temperatures, leaving some DPH in solution to rotate freely.

An important observation from the steady-state anisotropy data was that no phase transition could be observed for DPPC vesicles that were entrapped in TEOS derived glasses (see Figure 5). This result, along with the low anisotropy value (relative to the values in solution and other entrapped samples) and the increase in anisotropy with temperature strongly suggests that the liposomes may have ruptured within the TEOS based silica. Interestingly, no leaching of lipidic material was observed from these samples, and it is noteworthy that the anisotropy of DPH is much higher than would be expected is the probe were simply present in solution. Taken together, the data suggest that the lipids and DPH may have adsorbed onto the silica surface in the TEOS derived materials, producing an entrapped/adsorbed lipid system that was not able to undergo normal phase-transition behavior. This situation could be the result of interactions of the liposomes with ethanol that was produced during the hydrolysis of TEOS prior to the entrapment of the liposomes. The release of ethanol may simply disrupt the liposomal

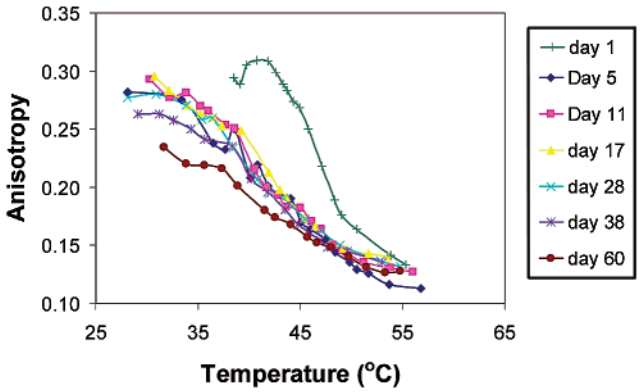

Figure 6. Phase-transition behavior of DPPC aged in 50 mM Tris HCl buffer pH 7.4, measured by the steady-state anisotropy of DPH, following entrapment in sodium silicate derived material.

TABLE 1: Time-Resolved Fluorescence Intensity Decay of DPH in DPPC Liposomes in Solution and Following Entrapment into Various Sol−Gel Derived Materials[a]

	solution	SSS	DGS	TEOS
τ_1 (ns)	2.75	2.00	2.81	1.19
τ_2 (ns)	8.65	10.00	9.20	8.95
f_1	0.08	0.06	0.04	0.09
f_2	0.92	0.94	0.96	0.91
χ^2	1.079	1.107	1.088	1.150

[a] Typical errors in lifetime values are ±0.05 ns; typical errors in fractional fluorescence values are ±0.01.

structure by partially dissolving the macromolecular structure. This suggests that TEOS is likely a poor precursor for entrapping liposomes due to the presence of ethanol, which has previously been shown to destabilize some proteins following entrapment.[62]

Figure 6 shows the effect of aging time on the phase-transition behavior of DPPC entrapped in sodium silicate glasses. It can be seen that over time a loss of the sinusoidal phase transition and a broadening of the phase transition occurs, with much of the change occurring within the first week. An overall decrease in anisotropy in the low-temperature range is seen as well, suggesting that the liposomes undergo irreversible structural alterations that lead to loss of phase-transition behavior. Similar results were observed for DPPC when entrapped in DGS (results not shown) and did not depend on whether the samples were aged in buffer or in air. This trend in anisotropy over time suggests that the liposomes likely ruptured and lost their intrinsic physical properties as aging proceeded and indicates that improved entrapment and aging methods will be needed to ensure long-term viability of entrapped liposomes.

Time-Resolved Fluorescence Measurements. Table 1 shows the fluorescence decay data obtained for DPH in DPPC liposomes upon entrapment of these species into various sol−gel derived materials. In all cases, the decay of intensity was best fit to a biexponential decay model, in agreement with previous studies of DPH lifetimes in liposomes.[53−55,63−66] The biexponential decay observed for DPH in membranes has been associated with formation of both ground and excited state dimers and reflects emission from closely spaced ^{1}Ag* and ^{1}Bu* excited states, which produce the long and short decay components, respectively. The short lifetime component has also been attributed to a dimeric form of DPH that distorts the symmetry of the ^{1}Ag* excited state such that decay occurs much more readily.[65]

As shown in Table 1, the fluorescence decay of DPH-doped liposomes within sol−gel derived glasses is never identical to that in solution, although in the case of DGS based glasses, the

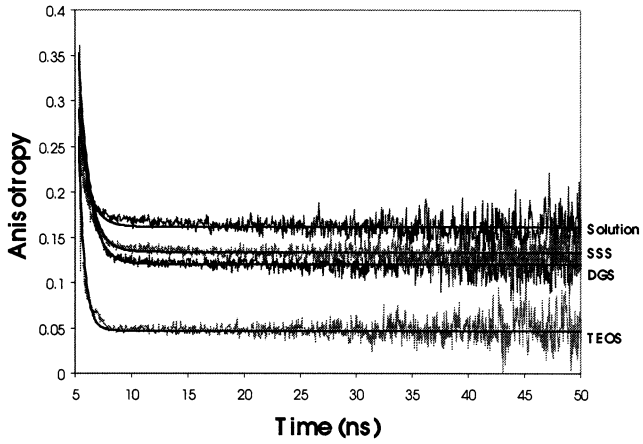

Figure 7. Time-resolved decay of fluorescence anisotropy of DPH in vesicles composed of DPPC in solution and following entrapment in sol−gel derived silica. The decay fits obtained from eq 2 are superimposed over the collected data.

TABLE 2: Time-Resolved Fluorescence Anisotropy Decay of DPH in DPPC Liposomes in Solution and Following Entrapment in Various Sol−Gel Derived Materials[a]

	ϕ (ns)	r_o	r_{inf}	θ_{max} (deg)	χ^2
solution	0.87	0.30	0.16	42	0.8717
DGS	0.95	0.35	0.12	54	1.0147
SSS	0.92	0.35	0.13	52	0.9968
TEOS	0.50	0.26	0.05	65	1.1270

[a] The constants ϕ, r_o, r_∞, and θ_{max} were obtained by fitting to eqs 4 and 5. Typical errors in rotational correlation times are ±0.05 ns; typical errors in θ_{max} values are ±2°.

values of the lifetime components are quite close to those in solution, suggesting similar environments for the DPH. The decay of DPH fluorescence in sodium silicate derived glasses shows a lengthening of the longer decay time, and a decrease in the value of the shorter decay time relative to solution, although the relative proportions of the two components are similar to those in solution. The physical basis for the changes in the decay time are difficult to interpret, but it is likely that the environment surrounding the DPH within the liposomes is somewhat different from that in solution, perhaps owing to some interaction of the liposomes with the silica surface. The decay of DPH in TEOS derived glasses shows a significant decrease of approximately 60% in the short lifetime component relative to solution, with the longer lifetime component remaining similar to that in solution. Given the previous anisotropy data, it is likely that the decrease in the short lifetime component reflects disruption of the lipid membrane structure, and thus may be a sensitive indicator of membrane perturbations upon entrapment.

Further insight into the behavior of DPH, and hence the structure of the membrane, is gained from analysis of the time-resolved fluorescence anisotropy. Figure 7 shows the anisotropy decay data obtained from DPH-doped liposomes in solution and in the different sol−gel derived glasses. It is clear that the anisotropy undergoes a rapid decay at early times owing to local motion of DPH within the bilayer but does not decay to zero at longer times, resulting in a significant residual anisotropy that is related to the slow rotational motion of the entire liposome, which is essentially immobile during the time scale of the DPH intensity decay. Table 2 shows the fits to the anisotropy decay data. A number of models were examined (multiexponential anisotropy decay, multicomponent hindered rotor), but the best fit to the data was obtained using a simple model of the anisotropic movement of DPH within a bilayer involving free rotation of a rigid rod within a cone symmetrically positioned

with its apex normal to the plane of the bilayer.[36,67] Using this model, the data in Table 2 reveal three critical pieces of information that may be used to describe the degree of constraint of DPH within the membrane. First, the rotational correlation time for the anisotropy decay is essentially the same in solution, DGS, and sodium silicate based glasses but is almost a factor of 2 faster in TEOS derived glasses. Second, the residual anisotropy of DPH (given by the r_∞ value) is slightly lower in DGS and sodium silicate glasses when compared with the value in solution, but again the value in TEOS derived glasses is substantially lower than in solution (~30% of the solution value). Third, the semi-angle for precession of DPH increases upon entrapment, indicative of greater mobility of the probe. For liposomes that were entrapped in DGS or SSS derived materials a maximum cone angle of about 53° is observed, which is approximately 10° larger than was observed in solution. However, liposomes entrapped in TEOS derived materials show a cone angle of 65°, which is 25° larger than that seen in solution. Taken together, these results confirm that entrapment of liposomes into all of the materials causes some degree of change in the liposome dynamics, but in the case of TEOS it is apparent that the DPH is no longer completely associated with the membrane and is nearly free to rotate without hindrance. Thus, our findings demonstrate that entrapment of liposomes using alkoxysilane derived materials can cause significant alterations in the structure of the liposome owing to interactions between the lipid and the alcohol that is liberated during hydrolysis of the precursor. However, the use of aqueous processing methods (as with sodium silicate) or glycerated silane precursors (which liberate glycerol upon hydrolysis) can alleviate these problems and produce viable entrapped liposomes.

Sol−Gel-Entrapped pH-Sensitive Liposomes. As a practical demonstration of the use phase transitions within immobilized membranes for sensing applications, we have examined the use of pH-induced perturbations of the phase equilibria of liposomes composed of 85% DPPC, 10% DPPA, and 5% NBD-PE. Previous studies have clearly demonstrated that pH- or pressure-induced alterations in the phase distribution within such systems can lead to significant changes in fluorescence intensity owing to changes in the degree of self-quenching of NBD-PE within the membrane.[68,69] In this system, the average concentration of NBD-PE is constant but is distributed between microscopic phases such that it partitions into the less ordered regions of the membrane. Changes in the surface charge that reduce electrostatic repulsions between headgroups lead to an overall contraction of the membrane and can also promote the formation of the more ordered phase.[68] In this case, the average area occupied by the NBD-PE molecules decreases, leading to enhanced self-quenching a thus a decrease in emission intensity. Conversely, ionization of the headgroups leads to expansion of the liposome and the formation of a greater amount of the disordered phase, increasing the average area occupied by NBD-PE and thus reducing self-quenching and increasing the emission intensity.

Figure 8 shows the pH profile for the DPPC/DPPA/NBD-PE liposomes as a function of pH both in solution and for liposomes entrapped in sodium silicate glasses. As the pH is made more basic, the DPPA headgroups become more ionized, leading to a net increase in the area occupied by the NDB-PE moieties. This has the expected effect of reducing the self-quenching and increasing the emission intensity. Inflections in the fluorescence intensity are seen at the characteristic pK_a values of DPPA (3.0 and 9.0),[70] indicating that the degree of ionization of the membrane is responsible for the alterations in pH. Similar experiments carried out with DPPC or egg PC vesicles in the absence of DPPA resulted in no changes in the fluorescence intensity of NBD-PE (results not shown), confirming that ionization of the membrane is necessary to produce this effect. It is also noteworthy that the net change in emission intensity is on the order of 6-fold over the pH range studied. This is a significantly greater change in intensity than is obtained from conventional pH indicator dyes such as fluorescein, and suggests that this strategy may have some utility in the sensing of small pH changes. It is also possible that phase transitions could be triggered using methods other than pH changes. For example, Krull and co-workers have demonstrated the reactions of enzymes with substrates,[41] antibodies with antigens,[71] and receptors with antagonists[72] all lead to changes in the intensity of NBD-PE-doped lipid membranes. Thus, it is possible that such reactions could also be monitored using sol−gel-immobilized liposomes to produce stable sensors.

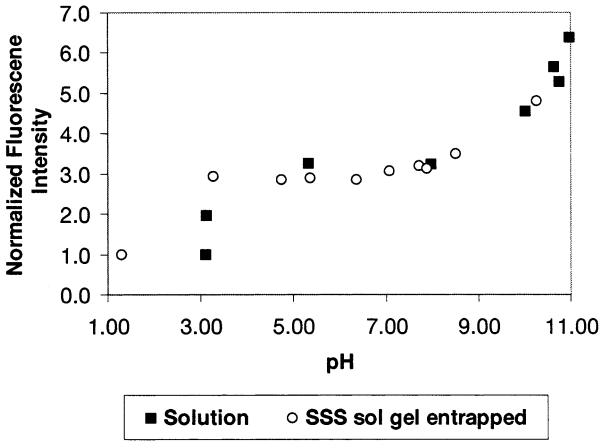

Figure 8. Change in fluorescence emission intensity of 5% NBD-PE, 10% DPPA to DPPC vesicles in response to changes in pH in solution and following entrapment in SSS. Emission intensities were normalized relative to the fluorescence change that occurred at the minimum pH value in either solution or SSS.

Conclusion

Phospholipid liposomes can be easily entrapped in sol−gel derived materials and show no leaching of lipid components over a period of many months when the samples are stored at moderate pH values. Entrapped liposomes generally retain their normal spherical shape after entrapment into sol−gel derived silica, although other structures that arise from vesicle fusion and/or rupture are possible. Steady-state and time-resolved fluorescence studies of DPH-doped liposomes demonstrate that liposomes can undergo significant changes in their dynamics and phase-transition behavior after entrapment into sol−gel derived silica, although the extent of these changes depends on the nature of the precursor used to form the silica material. Entrapment methods that utilize aqueous processing methods (as for sodium silicate) or glycerol based precursors produce liposomes that retain their native physical properties and phase-transition behavior over a period of several days, as opposed to conventional immobilization techniques where lipid bilayers or liposomes are stable for only a few hours.[2,3] However, entrapment using alkoxysilane precursors tends to cause large-scale changes in the liposome structure and dynamics and results in a system that does not display phase-transition behavior. The ability to maintain the dynamic motions of the bilayer lipid membrane after entrapment is likely to be a major advantage of this immobilization method, as it is likely that membrane

mobility is needed to maintain the activity of transmembrane receptors. The dynamic behavior can also be exploited to produce a sensing strategy based on alterations of self-quenching of an embedded dye, as demonstrated herein. These studies set the stage for further studies involving entrapped ion channels, receptors, and other membrane-bound species.

Acknowledgment. We thank the Natural Sciences and Engineering Research Council of Canada, MDS-Sciex, the Canada Foundation for Innovation, and the Ontario Innovation Trust for support of this work. J.D.B. holds the Canada Research Chair in Bioanalytical Chemistry.

References and Notes

(1) Tien, H. T.; Ottova, A. L. *Colloids Surf. A* **1999**, *149*, 217.
(2) Dong, S.; Chen, X. *Rev. Mol. Biotechnol.* **2002**, *82*, 303.
(3) Bernhard, S.; Sleytr, U. B. *Rev. Mol. Biotechnol.* **2000**, *74*, 233.
(4) Knoll, W.; et al. *Rev. Mol. Biotechnol.* **2000**, *74*, 137.
(5) Krull, U. J.; et al. *Talanta* **1990**, *37*, 561.
(6) Borenstain, V.; Barenholz, Y.; *Chem. Phys. Lipids* **1993**, *64*, 117.
(7) Watts, A. *Curr. Opin. Biotechnol.* **1999**, *10*, 48.
(8) Sebille, B.; et al. *J. Chromatogr.* **1990**, *531*, 51.
(9) Fang, Y.; Frutos, A. G.; Lahiri, J. *J. Am. Chem. Soc.* **2002**, *124*, 2394.
(10) Bianco, P. *Rev. Mol. Biotechnol.* **2002**, *82*, 393.
(11) Butkus, E.; et al. *J. Chem. Res.* **1998**, 722.
(12) Goa, H., et al. *J. Photochem. Photobiol. B* **2000**, *59*, 87.
(13) Kinji, A.; Ottova, A. L.; Tien, H. T. *Thin Solid Films* **1999**, *354*, 201.
(14) Snejdarkova, M.; et al. *Bioelectrochem. Bioenerg.* **1997**, *42*, 35.
(15) Snejdarkova, M.; Rehak, M.; Otto, M. *Anal. Chem*. **1993**, *65*, 665.
(16) Sugao, N.; et al. *Anal. Chem*. **1993**, *65*, 363.
(17) Brennan, J. D.; Kallury, K. M. R.; Krull, U. J. *Thin Solid Films* **1994**, *244*, 898.
(18) Brennan, J. D.; et al. *Anal. Chim. Acta* **1991**, *255*, 73.
(19) Krull, U. J.; Heimlich, M. S.; Kallury, K. M. R.; Piunno, P. A. E.; Brennan, J. D.; Brown, R. S.; Nikolelis, D. P. *Can. J. Chem.* **1995**, *73*, 1239.
(20) Osborn, T. D.; Yager, P. *Langmuir* **1995**, *11*, 8.
(21) Kallury, K. M. R.; Lee, W. E.; Thompson, M. *Anal. Chem.* **1992**, *64*, 1062.
(22) Peng, T.; Cheng, Q.; Stevens, R. C. *Anal. Chem.* **2000**, *72*, 1611.
(23) Percot, A.; Zhu, X. X.; Lafluer, M. *Biocong. Chem*. **2000**, *11*, 647.
(24) Boukobza, E.; Sonnenfeld, A.; Haran, G. *J. Phys. Chem. B* **2001**, *105*, 12165.
(25) Trojanowicz, M.; Miernik, A. *Electrochim. Acta* **2001**, *46*, 1053.
(26) Diao, P.; et al. *Bioelectrochem. Bioenerg.* **1998**, *45*, 173.
(27) Tien, H. T.; Wang, L.; Wang, X.; Ottova, A. L. *Bioelectrochem. Bioenerg.* **1997**, *42*, 161.
(28) Asaka, K.; Tien, H. T.; Ottova, A. L. *J. Biochem. Biophys. Methods* **1999**, *40*, 27.
(29) Hianik, T.; Snejdarkova, M.; Rehak, M.; *J. Bioelectrochem. Bioenerg.* **1997**, *39*, 235.
(30) Gao, H.; Feng, F.; Lou, G. *Electroanalysis* **2001**, *13*, 49.
(31) Yamada, H.; Shiku, H.; Tomokazu, M. *J. Phys. Chem*. **1993**, *97*, 9546.
(32) Lentz, B. R. *Chem. Phys. Lipids* **1993**, *64*, 99.
(33) Schuster, B.; Sleytr, U. B. *Rev. Mol. Biotechnol.* **2000**, *74*, 2.
(34) Gill, I. *Chem. Mater.* **2001**, *13*, 3404.
(35) Jin, W.; Brennan, J. D. *Anal. Chim. Acta* **2002**, *461*, 1.
(36) Sasaki, D. Y.; Shea, L. E.; Sinclair, M. B. *Proc. SPIE Int. Soc. Opt. Eng.* **1999**, *3062*, 275.
(37) Yamanaka, S. A.; Charych, D. H.; Loy, D. A.; Sasaki, D. Y. *Langmuir* **1997**, *13*, 5049.
(38) Ishiwatari, T.; Shimizu, I.; Mitsuishi, M. *Chem. Lett.* **1996**, 33.
(39) Nguyen, T.; McNamara, K. P.; Rosenzweig, Z. *Anal. Chim. Acta* **1999**, *400*, 45.
(40) Marsh, D. *CRC Handbook of Lipid Bilayers*; Chemical Rubber Company Press: Boca Raton, FL, 1990.
(41) Brennan, J. D.; Brown, R. S.; McClintock, C. P.; Krull, U. J. *Anal. Chim. Acta* **1990**, *237*, 253.
(42) Brook, M. A.; Brennan, J. D.; Chen, D. Y. U.S. Provisional Patent 60/384, 084, 2002.
(43) Bhatia, R. B.; Brinker, C. J.; Gupta, A. K.; Singh, A. K. *Chem. Mater.* **2000**, *12*, 2434.
(44) Flora, K. K.; Brennan, J. D. *J. Phys. Chem. B* **2001**, *103*, 12003.
(45) Knutson, J. R.; Beechem, J. M.; Brand, L. *Chem. Phys. Lett.* **1983**, *102*, 501.
(46) O'Connor, D. V.; Phillips, D. *Time-Correlated Single Photon Counting*; Academic Press: New York, 1984.
(47) Demas, J. N. *Excited-State Lifetime Measurements*; Academic Press: New York, 1983.
(48) Lakowicz, J. R.; Gryczynski, I. In *Topics in Fluorescence Spectroscopy*; Lakowicz, J. R., Ed.; Plenum: New York, 1991; Vol. 1, Chapter 5.
(49) Bright, F. V.; Betts, T. A.; Litwiler, K. S. *CRC Crit. Rev. Anal. Chem.* **1990**, *21*, 389.
(50) Bright, F. V. *Appl. Spectrosc*. **1995**, *49*, 14A.
(51) Verkleij, A. J.; Leunissen-Bijvelt, J.; De Kruijff, B.; Hope, M.; Cullis, P. R. *Ciba Found. Symp.* **1984**, *103*, 45.
(52) Cevc, G. *Biochim. Biophys. Acta* **1991**, *1062*, 59.
(53) Lentz, B. R. *Chem. Phys. Lipids* **1989**, *50*, 171.
(54) Van Der Meer, W., et al. *Biophys. J*. **1984**, *46*, 515.
(55) Ameloot, M., et al. *Biophys. J*. **1984**, *46*, 525.
(56) Zheng, L.; Brennan, J. D. *Analyst* **1998**, *123*, 1735.
(57) Zheng, L.; Flora, K. K.; Brennan, J. D. *Chem. Mater*. **1998**, *10*, 3974.
(58) Brennan, J. D. *Appl. Spectrosc.* **1999**, *53*, 106A.
(59) Eggers, D. K.; Valentine, J. S. *Protein Sci.* **2001**, *10*, 250.
(60) Zhou, H.-X.; Dill, K. A. *Biochemistry* **2001**, *40*, 11289.
(61) Gaines, G. *Insoluble Monolayers at Liquid−Gas Interfaces*; Interscience Publishers: New York, 1966.
(62) Gill, I.; Ballesteros, A. *J. Am. Chem. Soc*. **1998,** *120*, 8587.
(63) Chen, L. A.; Dale, R. E.; Roth, S.; Brand, L. *J. Biol. Chem*. **1977**, *252*, 2163.
(64) Parasassi, T.; Conti, F.; Glaser, M.; Gratton, E. *J. Biol. Chem* **1984**, *259*, 14011.
(65) Kinosita, K.; Ikegami, A. *Biochim. Biophys. Acta* **1984**, *769*, 523.
(66) Chundall, R. B.; et al. *Chem. Phys. Lett.* **1979**, *64*, 39.
(67) Kinosita, K., Jr.; Kawato, S.; Ikegami, A. *Biochemistry* **1977**, *16*, 2319.
(68) Brennan, J. D.; Brown, R. S.; Krull, U. J. *Anal. Sci.* **1998**, *14*, 141.
(69) Brown, R. S.; Brennan, J. D.; Krull, U. J. *J. Chem Phys*. **1994**, *100*, 6019.
(70) Eibl, H.; Blume, A. *Biochim. Biophys. Acta* **1979**, *553*, 476.
(71) Wang, H.; Brennan, J. D.; Gene, A.; Krull, U. J. *Appl. Biochem. Biotechnol.* **1995**, *53*, 163.
(72) Krull, U. J.; Brennan, J. D.; Brown, R. S.; Hosein, S.; Hougham, B. D.; Vandenberg, E. T. *Analyst* **1990**, *115*, 147.